Phonon-Assisted Resonant Magnetotunneling in AlGaAs-GaAs-AlGaAs Heterostructures

Nanzhi Zou* and K. A. Chao
Division of Physics, Department of Physics and Mathematics, Norwegian Institute of Technology, The University of Trondheim, N 7034 Trondheim, Norway

Yu. M. Galperin
Department of Physics, University of Oslo, P.O. Box 1048 Blindern, N 0316 Oslo 3, Norway and A. F. Ioffe Physico-Technical Institute, 194021 St. Petersburg, Russia
(Received 8 February 1993)

The theory of inelastic electron resonant tunneling through a double-barrier nanostructure is extended to establish a theory of phonon-assisted resonant magnetotunneling when a magnetic field is applied parallel to the tunneling current. At higher temperatures we have discovered an interesting characteristic oscillation of the width and height of the main peak in the *I-V* curve when the ratio ω_0/ω_c changes between integer (*double resonant*) and half integer (*single resonant*), where ω_0 is the LO phonon frequency and ω_c is the cyclotron frequency in the well. If confirmed experimentally, our theoretical prediction provides an additional method to determine the electronic effective mass in the well.

PACS numbers: 71.38.+i, 72.10.Di, 73.40.Kp

Resonant tunneling through heterostructures under a magnetic field **B** has both intrinsic theoretical interest and great potential in device applications. Recent investigations have focused on the case **B**∥**I**, where **I** is the tunneling current. *I-V* characteristics and *I-B* curves have been measured on different types of $GaAs/Al_xGa_{1-x}As$ samples with geometric structures of single barrier [1–3], double barrier [4–17], triple barrier [18], laterally restricted double barrier [19], quantum dots [20], superlattice [21], and Coulomb island [22]. The magnetic field enhances the peak-to-valley ratio which is important for device performance. In the resonant regime, from the magneto-oscillation one can deduce the effective mass, the charge buildup in the well, and the dimensionality (2D or 3D) of the emitter.

As a general problem for transport properties, inelastic scatterings complicate the experimental data. Therefore, except for a few attempts based on simplified models [23–26], there exists no realistic theoretical study on inelastic resonant magnetotunneling through heterostructures. In high quality samples where scatterings due to impurities and interface imperfections can be much suppressed, electron-LO phonon interaction is the dominating inelastic scattering channel. Phonon-assisted tunneling through double-barrier resonant-tunneling (DBRT) structures has been thoroughly studied both experimentally and theoretically. Therefore, it is natural to extend such experiments to measure the phonon-assisted resonant magnetotunneling (PARMT) in those high quality samples [11–17]. Among various interesting phenomena exhibited in these PARMT data, magnetopolarons are observed if the electron system in the emitter is 2D [14,15].

The purpose of this Letter is not to propose ambitiously a complete theory, but to present a thorough treatment of the effect of phonons, with emphasis on an extremely important case when the ratio ω_0/ω_c of the LO phonon frequency ω_0 to the cyclotron frequency ω_c is an integer. This *double-resonant* tunneling will lead to the formation of magnetopolarons at low temperature which has been observed [14,15]. At finite temperature, our theoretical calculation shows that when the electron system in the emitter is 2D, the *double resonant* modifies drastically the main peak of the *I-V* characteristics, from which the cyclotron effective mass electron in the well can be deduced. To our knowledge, such finite temperature feature is predicted here for the first time, and remains to be confirmed by future experiments.

The DBRT structure is shown schematically in Fig. 1 with conventional terminology. The magnetic field **B** is perpendicular to interfaces which are assumed perfect and define the *x-y* plane. The electron states in both the emitter at the left and the collector at the right are specified by the set of quantum numbers $\beta=(n,k_y,k_\perp)$

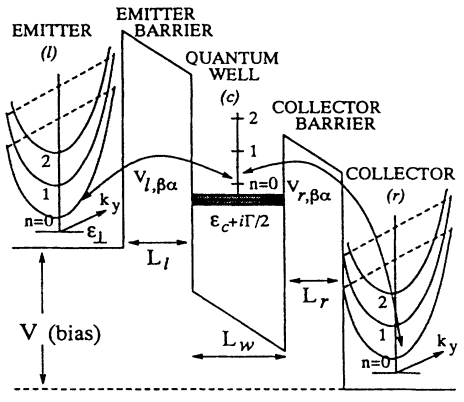

FIG. 1. A schematic illustration of the PARMT through a GaAs-AlGaAs DBRT structure.

0031-9007/93/71(11)/1756(4)$06.00

with corresponding energy $\epsilon_\beta=\epsilon_\perp+(n+\frac{1}{2})\hbar\omega_c$, where $\epsilon_\perp\equiv\hbar^2k_\perp^2/2m^*$. The electron states in the well are specified by the set of quantum numbers $\alpha=(n,k_y)$ with corresponding energy $E_\alpha=\epsilon_c+(n+\frac{1}{2})\hbar\omega_c$. We then consider the model Hamiltonian $\mathcal{H}=\mathcal{H}_{\rm el}+\mathcal{H}_{\rm ph}+\mathcal{H}_s$ in which the electronic part is

$$\mathcal{H}_{\rm el}=\sum_{j,\beta}\epsilon_\beta c_{j,\beta}^\dagger c_{j,\beta}+\sum_\alpha E_\alpha c_\alpha^\dagger c_\alpha + \sum_{j,\alpha,\beta}[V_{j,\beta\alpha}c_\alpha^\dagger c_{j,\beta}+\text{H.c.}]\,, \tag{1}$$

where $j=l$ (or r) refers to the left emitter (or right collector). In order to obtain quantitative results, we restrict ourselves to the bulk LO phonon Hamiltonian $\mathcal{H}_{\rm ph}=\sum_q\hbar\omega_{\mathbf{q}}b_{\mathbf{q}}^\dagger b_{\mathbf{q}}$. The role of confined or interface phonon modes will be discussed later qualitatively. For PARMT, the relevant electron-LO phonon interaction occurs when the electron occupies the state in the well. This interaction is expressed in terms of the Frölich Hamiltonian

$$\mathcal{H}_s=\sum_{\alpha,\alpha',\mathbf{q}}\frac{M}{\sqrt{V_0}q}\langle\alpha'|e^{i\mathbf{q}\cdot\mathbf{r}}|\alpha\rangle(b_{\mathbf{q}}^\dagger+b_{-\mathbf{q}})c_{\alpha'}^\dagger c_\alpha\,, \tag{2}$$

where $\alpha=(n,k_y)$, $\alpha'=(n',k_y-q_y)$, and $M^2=2\pi e^2\hbar\omega_0\times(1/\epsilon_\infty-1/\epsilon_0)$.

Since the interfaces are assumed perfect, within the effective mass approximation, for a given DBRT structure and a given bias, the quasibound state energy $\epsilon_c+i\Gamma/2$, $V_{l,\beta\alpha}$ and the matrix elements $V_{r,\beta\alpha}$ in Fig. 1 (or in $\mathcal{H}_{\rm el}$) can be computed from a one-dimensional Schrödinger equation [27]. In the absence of an external magnetic field, if we neglect the *electron recoil* (within the framework of the linear model [28]), then all LO phonon modes have been derived numerically and used to calculate the phonon replicas, which agree excellently with experimental results [29]. When the *electron recoil* is taken into account, the inelastic electron tunneling should be analyzed with three-dimensional phonon dispersion. In this case we will neglect the weak dispersion of the LO phonons and use the approximated phonon Hamiltonian $\mathcal{H}_{\rm ph}\simeq\hbar\omega_0\sum_{\mathbf{q}}b_{\mathbf{q}}^\dagger b_{\mathbf{q}}$ in order to produce quantitative results [30]. The mathematical analysis for the present work on PARMT including the *electron recoil* is very similar to that used in Ref. [30]. Therefore, we will present here only the key formulas.

Within the *wide band approximation* [28] $\sum_\beta|V_{j,\beta\alpha}|^2\times\delta(\epsilon_\beta-\epsilon)\simeq\Gamma_j$ which is energy independent, the total transmission probability of an electron tunneling from the emitter ($j=l$) to the collector ($j=r$) with energy $\epsilon=\epsilon_\perp+(n+\frac{1}{2})\hbar\omega_c$ can be expressed as

$$T_{\rm tot}(\epsilon_\perp,n)=\Gamma_l\Gamma_r\sum_{\alpha'}\int ds\,dt\,e^{i\epsilon(t-s)}\Theta(s)\Theta(t)\langle c_\alpha(t-s)c_{\alpha'}^\dagger(t)c_{\alpha'}(t)c_\alpha^\dagger(0)\rangle\,. \tag{3}$$

The Green's function is calculated with the Matsubara technique analytically continued to the complex energy plane. $T_{\rm tot}(\epsilon_\perp,n)$ contains both the intra-Landau-level tunneling $T(\epsilon_\perp-\epsilon_c)$ and the phonon-assisted inter-Landau-level tunneling $T[\epsilon_\perp-\epsilon_c+(n-n')\hbar\omega_0\pm\hbar\omega_c]$, where $T(\epsilon)=4\Gamma_l\Gamma_r/[4\epsilon^2+(\Gamma_l+\Gamma_r)^2]$.

At higher temperature we have discovered another interesting observable phenomenon in connection to the *double resonant* condition $(n-n')\hbar\omega_c=\hbar\omega_0$. In order to demonstrate our important finding, we have performed detailed numerical calculations with a realistic GaAs/$Al_{0.3}Ga_{0.7}As$ DBRT sample of barrier width 4 nm and well width 5 nm. In our earlier works [27,29,30] one finds the values of all material parameters and computation procedure, which is general for a 3D emitter. If the emitter is 2D, the calculation of tunneling current is even simpler because the integration over $\epsilon_\perp$ can be ignored. Our calculation $T_{\rm tot}(\epsilon_\perp,n=0)$ at temperature $T=200$ K is shown in Fig. 2. Besides the main peak (marked as M) and the usual phonon replica (intra-Landau-level tunneling with the emission of one phonon, marked as Ph-R), we also see the inter-Landau-level PARMT with both phonon emission (marked as $E_{0,n'}$) and phonon absorption (marked as $A_{0,n'}$). When the *double resonant* condition $\omega_0/\omega_c=\nu=$integer is satisfied, both the pure intra-Landau-level resonant tunneling and the phonon-absorption inter-Landau-level resonant tunneling occur simultaneously, and consequently the main peak and the $A_{0,\nu}$ peak merge into a broadened peak. The width of this broadened peak grows with magnetic field strength. With increasing magnetic field, as ω_0/ω_c passes the integer ν, we see first the $A_{0,\nu}$ peak merging into the main peak, and then the $A_{0,\nu+1}$ peak emerging out of the main peak.

Knowing the transmission probability, for given bias V and given electron system in the emitter (ESE), we can calculate the tunneling current I [29,30]. If the ESE is 2D, we found many interesting features, which become much less distinct if the ESE is 3D, because in this case the energy spectrum is no longer completely discrete, and one needs to integrate over $\epsilon_\perp$. In the following we report the most important new result derived with a 2D ESE of realistic electron density 4×10^{11} cm^{-2}. For a 2D ESE the potential curve in Fig. 1 contains a pseudotriangle well (not shown in the figure) in the emitter region. Since the resultant single-electron potential in Fig. 1 depends on the bias, both quasibound energy levels in the pseudotriangle well and in the middle quantum well also depend on the bias. Such a feature has been taken into account in our calculation. Corresponding to Fig. 2, the main peak in the I-V curve at temperature 200 K is shown in Fig. 3 for *double resonant* cases $\omega_0/\omega_c=1.0$ and 2.0, as well as for *single resonant* cases $\omega_0/\omega_c=1.5$ and 2.5. The general feature is that between two *double resonant* cases $\omega_0/\omega_c=\nu$ and $\nu+1$, the peak for *single resonant* tunneling $\omega_0/\omega_c=\nu+\frac{1}{2}$ is the sharpest one with the largest peak current.

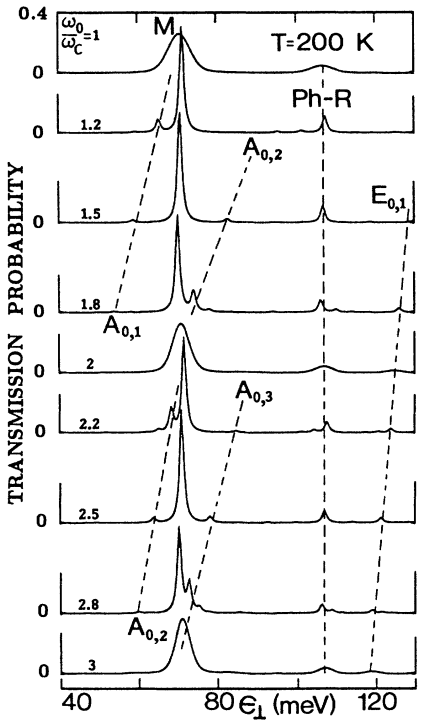

FIG. 2. Finite temperature electron transmission probability $T_{\rm tot}(\epsilon_\perp, n=0)$ exhibiting the characteristic features of *double resonant tunneling.*

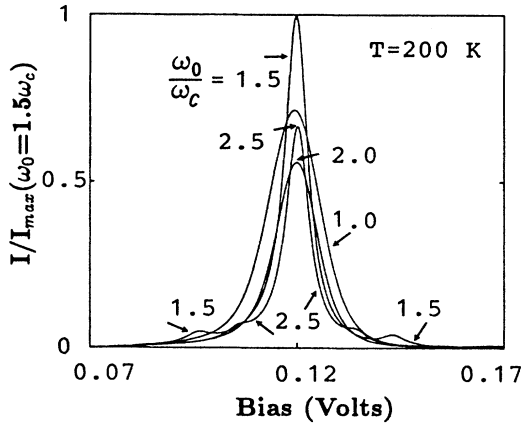

FIG. 3. Normalized current $I/I_{\rm max}(\omega_c=\omega_0)$ as a function of the bias at the temperature 200 K, for the ratio ω_0/ω_c varying between *double resonant* values and *single resonant* values.

The results in Fig. 3 indicate the interesting oscillation in the width and height of the main resonant current peak, a modulation of transmission spectrum at high temperatures via magnetic field induced double resonant tunneling. In order to determine the experimental conditions under which this new phenomenon can be observed, besides the above-mentioned bias dependence of the single-electron potential and the quasibound energy levels, we must specify one more point concerning the 2D ESE used in our calculation. It is known that the sheet electron concentration n_s of the 2D ESE also changes with the applied bias. Since all peaks in Fig. 3 occur at almost the same bias, say V_p, to reduce the uncertainty caused by the variation of n_s, when the bias changes, we will try to set the bias at V_p and detect experimentally the oscillation of the peak height with a sweep of the magnetic field strength B. At this fixed bias, the possible change of n_s with B is expected to be a secondary effect, and is too weak to destroy the predicted oscillation. With the bias V_p for maximum resonant-tunneling current, in our calculation, the upper bound of n_s is restricted by the condition that for a given B and a given temperature, only the lowest Landau level is heavily populated, while the populations in all higher Landau levels are negligibly small. At the temperature 200 K, this condition is satisfied with our choice $n_s=4\times10^{11}$ cm^{-2}, provided that $B>12$ T.

With only the lowest Landau level in the 2D ESE populated, the electron effective mass in the 2D ESE is not important to the condition of observation. On the other hand, higher Landau levels in the well are involved in the *double resonant* tunneling. Taking into account the nonparabolicity effect [31], we found the corresponding variation of the effective mass of electrons in the well to be less than 7%. Consequently, our predicted modulation of peak height is observable at higher temperatures. Again, since the cyclotron frequency ω_c appeared in Fig. 3 is associated to the electrons in the well, our theoretical prediction, if confirmed experimentally, provides an additional method to measure the electronic effective mass in the quantum well with a small error of a few percents.

While at higher temperature the required coherence for the formation of magnetopolarons is destroyed by the electron-LO photon interaction, it is restored at very low temperature and so two Landau levels are strongly hybridized in the *anticrossing region* where $(n-n')\hbar\omega_c-\hbar\omega_0$ is small. In this case electrons tunnel primarily through two hybridized states which are created by the operators

$$A^\dagger_{k_y,+}=u_{k_y}c^\dagger_{n,k_y}+\sum_{\mathbf{q}}v_{k_y,\mathbf{q}}b^\dagger_{\mathbf{q}}c^\dagger_{n',k_y-q_y}$$

and

$$A^\dagger_{k_y,-}=u^*_{k_y}c^\dagger_{n',k_y-q_y}-\sum_{\mathbf{q}}v^*_{k_y,\mathbf{q}}b_{\mathbf{q}}c^\dagger_{n,k_y}\,.$$

Our calculation of tunneling current can be largely simplified by incorporating these two hybridized states into (3). Here in Fig. 4 we only plot $T_{\rm tot}(\epsilon_\perp,n=1)$ to show that the peak width for $\omega_0/\omega_c=1$ at low temperature is much narrower than those at higher temperatures given in Fig. 2 for $\omega_0/\omega_c=$integer.

In our calculation we have considered only the bulk LO phonon modes which lead to the $\sqrt{B}$ dependence of the replica intensity. One can easily show that the same $\sqrt{B}$ dependence holds also for interface modes under the usu-

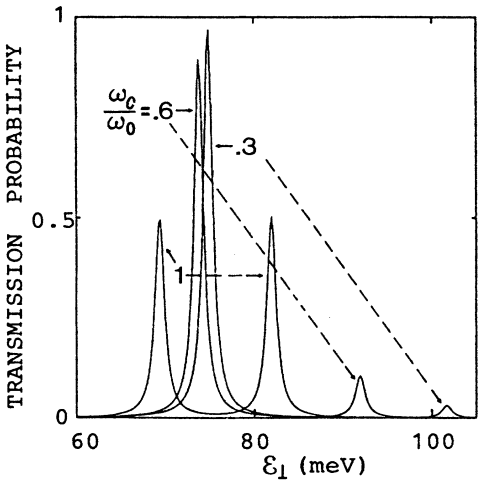

FIG. 4. Zero temperature electron transmission probability $T_{\rm tot}(\epsilon_\perp, n=1)$ exhibiting the characteristic features of *anticrossing.*

al experimental condition $L_w \ll l = \sqrt{c\hbar/eB}$. On the other hand, for LO phonon modes confined in the well, the effective values of q_z are of the order of $1/L_w \gg 1/l$. This situation is similar to the impurity elastic scattering and therefore the magnetic field dependence should be proportional to B [32]. All these phonon modes can be included in our calculation without difficulty if their dispersions are negligibly weak.

The present work is supported by the Norwegian Research Council for Science and the Humanities (NAVF) Grant No. RT/SDU 424.90/009.

*Present address: Department of Physics and Measurement Technology, University of Linköping, S 58183 Linköping, Sweden.

[1] T. W. Hickmott, Phys. Rev. B **32**, 6531 (1985).
[2] E. Böckenhoff, K. v. Klitzing, and K. Ploog, Phys. Rev. B **38**, 10120 (1988).
[3] J. Smoliner, E. Gornik, and G. Weimann, Phys. Rev. B **39**, 12937 (1989).
[4] E. E. Mendez, L. Esaki, and W. I. Wang, Phys. Rev. B **33**, 2893 (1986).
[5] V. J. Goldman, D. C. Tsui, and J. E. Cunningham, Phys. Rev. B **35**, 9387 (1987).
[6] L. Eaves, G. A. Toombs, F. W. Sheard, C. A. Payling, M. L. Leadbeater, E. S. Alves, T. J. Foster, P. E. Simmonds, M. Henini, O. H. Hughes, J. C. Portal, G. Hill, and M. A. Pate, Appl. Phys. Lett. **52**, 212 (1988).
[7] D. Thomas, F. Chevoir, P. Bois, E. Barbier, Y. Guldner, and J. P. Vieren, Superlattices Microstruct. **5**, 219 (1989).
[8] S. Ben Amor, K. P. Martin, J. J. L. Rascol, R. J. Higgins, R. C. Potter, A. A. Lakhani, and H. Hier, Appl. Phys. Lett. **54**, 1908 (1989).
[9] A. Zaslavsky, D. C. Tsui, M. Santos, and M. Shayegan, Phys. Rev. B **40**, 9829 (1989).
[10] L. Eaves, M. L. Leadbeater, D. C. Mayes, E. S. Alves, F. W. Sheard, G. A. Toombs, P. E. Simmonds, M. S. Skolnick, M. Henini, and O. H. Hughes, Solid State Electron. **32**, 1101 (1989).
[11] M. L. Leadbeater, E. S. Alves, L. Eaves, M. Henini, O. H. Hughes, A. Celeste, J. C. Portal, G. Hill, and M. A. Pate, Phys. Rev. B **39**, 3438 (1989).
[12] C. H. Yang, M. J. Yang, and Y. C. Kao, Phys. Rev. B **40**, 6272 (1989).
[13] A. Celeste, L. A. Cury, J. C. Portal, M. Allovon, D. K. Maude, L. Eaves, M. Davies, M. Heath, and M. Maldonado, Solid State Electron. **32**, 1191 (1989).
[14] G. S. Boebinger, A. F. J. Levi, S. Schmitt-Rink, A. Passner, L. N. Pfeiffer, and K. W. West, Phys. Rev. Lett. **65**, 235 (1990).
[15] J. G. Chen, C. H. Yang, M. J. Yang, and R. A. Wilson, Phys. Rev. B **43**, 4531 (1991).
[16] Y. G. Gobato, F. Chevoir, J. M. Berroir, P. Bois, Y. Guldner, J. Nagle, J. P. Vieren, and B. Vinter, Phys. Rev. B **43**, 4843 (1991).
[17] R. E. Pritchard, P. C. Harness, L. Cury, J. C. Portal, B. Khamsehpour, W. S. Truscott, and K. E. Singer, Semicond. Sci. Technol. **6**, 626 (1991).
[18] J. J. L. Rascol, K. P. Martin, S. Ben Amor, R. J. Higgins, A. Celeste, J. C. Portal, A. Torabi, H. M. Harris, and C. J. Summers, Phys. Rev. B **41**, 3733 (1990).
[19] S. Tarucha and Y. Hirayama, Phys. Rev. B **43**, 9373 (1991).
[20] M. Tewordt, L. Martin-Moreno, V. J. Law, M. J. Keely, R. Newbury, M. Pepper, D. A. Ritchie, J. E. F. Frost, and G. A. C. Jones, Phys. Rev. B **46**, 3948 (1992).
[21] W. Müller, H. T. Grahn, R. J. Haug, and K. Ploog, Phys. Rev. B **46**, 9800 (1992).
[22] B. Su, V. J. Goldman, and J. E. Cunningham, Superlattices Microstruct. **12**, 305 (1992).
[23] C. E. T. Goncalves da Silva and E. E. Mendez, Phys. Rev. B **38**, 3994 (1988).
[24] P. A. Schulz and C. Tejedor, Phys. Rev. B **41**, 3053 (1990).
[25] W. Pötz, Phys. Rev. B **41**, 12111 (1990).
[26] P. J. Turley and S. W. Teitsworth, Phys. Rev. B **44**, 12959 (1991).
[27] Nanzhi Zou, J. Rammer, and K. A. Chao, Phys. Rev. B **46**, 15912 (1992).
[28] N. S. Wingreen, K. W. Jacobsen, and J. W. Wilkins, Phys. Rev. B **40**, 11834 (1989).
[29] Nanzhi Zou, J. Rammer, and K. A. Chao, Int. J. Mod. Phys. B (to be published).
[30] Nanzhi Zou and K. A. Chao, Phys. Rev. Lett. **69**, 3224 (1992).
[31] U. Ekenberg, Phys. Rev. B **40**, 7714 (1989).
[32] S. Das Sarma, Phys. Rev. Lett. **52**, 859 (1984); **52**, 1570(E) (1984).